Atmospheric Chemistry

DOI: 10.1002/anie.201408566

Rapid Autoxidation Forms Highly Oxidized RO_2 Radicals in the Atmosphere**

*Tuija Jokinen, Mikko Sipilä, Stefanie Richters, Veli-Matti Kerminen, Pauli Paasonen, Frank Stratmann, Douglas Worsnop, Markku Kulmala, Mikael Ehn, Hartmut Herrmann, and Torsten Berndt**

Abstract: *Gas-phase oxidation routes of biogenic emissions, mainly isoprene and monoterpenes, in the atmosphere are still the subject of intensive research with special attention being paid to the formation of aerosol constituents. This laboratory study shows that the most abundant monoterpenes (limonene and α-pinene) form highly oxidized RO_2 radicals with up to 12 O atoms, along with related closed-shell products, within a few seconds after the initial attack of ozone or OH radicals. The overall process, an intramolecular ROO→QOOH reaction and subsequent O_2 addition generating a next R′OO radical, is similar to the well-known autoxidation processes in the liquid phase (QOOH stands for a hydroperoxyalkyl radical). Field measurements show the relevance of this process to atmospheric chemistry. Thus, the well-known reaction principle of autoxidation is also applicable to the atmospheric gas-phase oxidation of hydrocarbons leading to extremely low-volatility products which contribute to organic aerosol mass and hence influence the aerosol–cloud–climate system.*

Autoxidation processes, that is, the oxidation of hydrocarbons by atmospheric oxygen, take place readily in the liquid phase, and such processes have been known since their discovery in 1875.[1] In this free-radical-chain process, once a free alkyl radical is formed by any initiation step, it reacts with O_2 and forms an RO_2 radical. The RO_2 radical then undergoes inter- or intramolecular H-abstraction, producing a hydroperoxide and the next alkyl radical that can propagate the chain process. Further reactions of the hydroperoxides lead to alcohols, aldehydes, ketones, and carboxylic acids.[2]

Autoxidation processes have been thought to be unimportant for the atmospheric gas-phase oxidation of hydrocarbons. This is because the chain propagation via intermolecular H-abstraction is highly unlikely due to the very low concentrations of hydrocarbons in the atmosphere (at most only a few ppbV). Furthermore, the intramolecular H-shift reaction, ROO→QOOH, becomes important only if relatively weak C–H bonds are available in the molecule, and then it is competitive with bimolecular reactions of the RO_2 radicals with NO, HO_2, and other RO_2 radicals (QOOH stands for a hydroperoxyalkyl radical).[3] Very recently, Ehn et al.[4] observed the formation of extremely low-volatility organic compounds (ELVOCs) from atmospheric measurements in a boreal forest and from the oxidation of α-pinene in a smog chamber. The ELVOCs are believed to contain OOH groups and their means of formation was assumed to be similar to an autoxidation process.

In this study, we performed comprehensive measurements of the oxidation products from the ozonolysis of limonene and α-pinene (including the OH radical reaction) over a wide range of alkene concentrations (atmospheric and higher) in an atmospheric-pressure flow tube.[5] Product formation (radicals and closed-shell species) was followed by means of NO_3^--CI-APi-TOF mass spectrometry,[6] which has been used to efficiently detect highly oxidized compounds as NO_3^- adducts.[4b] A detailed description of the experimental approach is given in the Supporting Information.

Figure 1 shows the concentrations of the most abundant RO_2 radicals (in red) and the closed-shell products (in black and blue) formed during ozonolysis experiments of the studied monoterpenes in our flow tube. Identical signals with the same elemental composition were detected from limonene and α-pinene due to the structural similarity of the reactants. For limonene, the attack of ozone takes place predominantly on the endocyclic double bond,[7,8] and for α-pinene it is the only reactive site. The formation of closed-shell C_{10} and C_{20} products (called monomers and dimers, respectively) appeared to be more effective in the limonene system than in the α-pinene system for a given RO_2 concentration level. The complete set of product spectra from both alkenes is given in Figure S1. Since OH radicals are inevitably formed in the course of the gas-phase ozonolysis of alkenes through the unimolecular decomposition of Criegee intermediates,[9] the product spectra comprise signals of the products formed in the OH radical–monoterpene reaction as well. A distinction was made possible in later experiments by applying OH radical scavengers.

[*] T. Jokinen, S. Richters, Dr. F. Stratmann, Prof. H. Herrmann, Dr. T. Berndt
Leibniz-Institut für Troposphärenforschung, TROPOS
04318 Leipzig (Germany)
T. Jokinen, Dr. M. Sipilä, Prof. V.-M. Kerminen, Dr. P. Paasonen, Dr. D. Worsnop, Prof. M. Kulmala, Dr. M. Ehn
Department of Physics, P.O. Box 64
00014 University of Helsinki (Finland)
Dr. D. Worsnop
Aerodyne Research Inc., Billerica, Massachusetts 01821 (USA)

[**] We thank K. Pielok, R. Gräfe, and A. Rohmer for technical assistance and the tofTools team for providing data analysis software. This work was funded in part by the European Commission (FP7-ENV-2010-265148), Academy of Finland (CoE project 1118615 and project 251427), and European research council (ATMNUCLE, grant 227463).

Supporting information for this article is available on the WWW under http://dx.doi.org/10.1002/anie.201408566.

 © 2014 Wiley-VCH Verlag GmbH & Co. KGaA, Weinheim

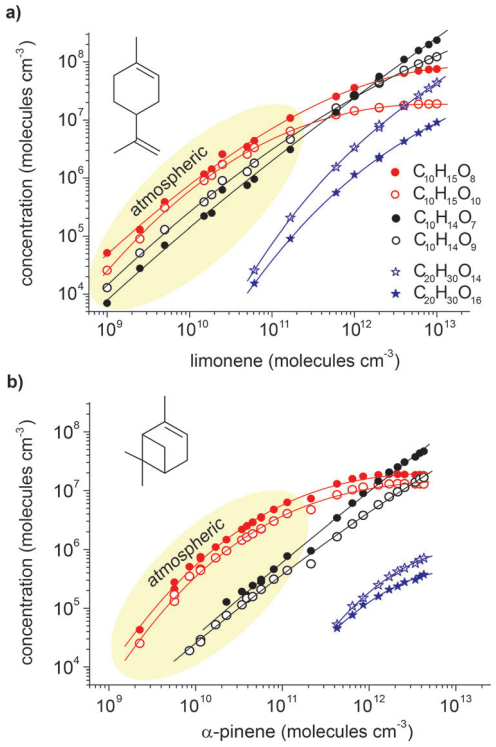

Figure 1. Concentrations of selected, highly oxidized products from the ozonolysis of a) limonene and b) α-pinene as a function of the alkene concentration; $[O_3] = 6.5 \times 10^{11}$ molecules cm^{-3}, reaction time 39.5 s. In red, the most abundant RO_2 radicals $C_{10}H_{15}O_8$ and $C_{10}H_{15}O_{10}$ (O,O-$C_{10}H_{15-x}(OOH)_xO_2$ for $x = 2$ and 3); in black, the closed-shell products $C_{10}H_{14}O_7$ and $C_{10}H_{14}O_9$ (monomers); and in blue, the dimers $C_{20}H_{30}O_{14}$ and $C_{20}H_{30}O_{16}$.

The signals assigned to RO_2 radicals were confirmed in experiments with NO addition in which the known products from the $RO_2 + NO_x$ reaction, organic nitrates and peroxynitrates, were detected.[10] $RONO_2$ formation yields of 32% and 27% ($RO_2 + NO \rightarrow RONO_2$) were determined for the two most abundant RO_2 radicals, $C_{10}H_{15}O_8$ and $C_{10}H_{15}O_{10}$, respectively (see Figure S2 in the Supporting Information).

A series of experiments with limonene were conducted to gain deeper insight into the formation of the highly oxidized products. First, the ozonolysis reaction was performed using either heavy ozone ($^{18}O_3$) or regular ozone ($^{16}O_3$) (see Figure S3). When $^{18}O_3$ was used instead of $^{16}O_3$, all the main peaks shifted by four mass units indicating that two O atoms from the attacking ozone are bound in these products. We reported a similar finding earlier for α-pinene ozonolysis in our flow tube.[4b] The oxidation products from the ^{18}OH-initiated reaction with limonene are expected to show a shift by two mass units (products from OH addition on limonene) compared to the products from the ^{16}OH reaction. These peaks were found by comparing the $^{18}O_3/^{16}O_3$ mass spectra, but they had low intensities. The detected signals with odd mass-to-charge numbers and two O atoms from the attacking ozone are consistent with the RO_2 radical formula O,O-$C_{10}H_{15-x}(OOH)_xO_2$, $x = 1$–4, showing differences of 31.9898 Th (two O atoms) each ("O,O" stands for two O atoms arising from ozone; the Thomson (Th) unit, which is not recognized by IUPAP or IUPAC, is a unit of *m/z*, where 1 Th = 1 u/e). Their formation can be explained by starting from the Criegee intermediates **2a** and **2b** after splitting off OH (Scheme 1a). The formed alkyl radicals **3a**–**3c** react with O_2 producing the corresponding RO_2 radicals **4a**–**4c**. Subsequent progress of the autoxidation process, that is, intramolecular H abstraction and subsequent O_2 addition, results in an increase in x. Scheme 1b shows an example of this reaction sequence starting from **4c**.

The relatively weak signals attributed to the OH-initiated RO_2 formation are consistent with the formula HO–$C_{10}H_{16-x}(OOH)_xO_2$, $x = 2$–4, again with a difference of 31.9898 Th between successive members in the series. The initial steps of the OH radical reaction with limonene are shown in Scheme 1c. The further autoxidation process proceeds in analogy to the reaction of **4c** in Scheme 1b. Our experiments in the absence/presence of OH radical scavenger (H_2 or C_3H_8) confirmed the assignment of the RO_2 radicals either to ozonolysis or to the OH-driven formation (Figure 2): only the signals attributed to HO–$C_{10}H_{16-x}(OOH)_xO_2$ radicals from the OH-initiated oxidation decreased in the presence of H_2 or C_3H_8, whereas the O,O-$C_{10}H_{15-x}(OOH)_xO_2$ radical signals from the ozonolysis remained unaffected.

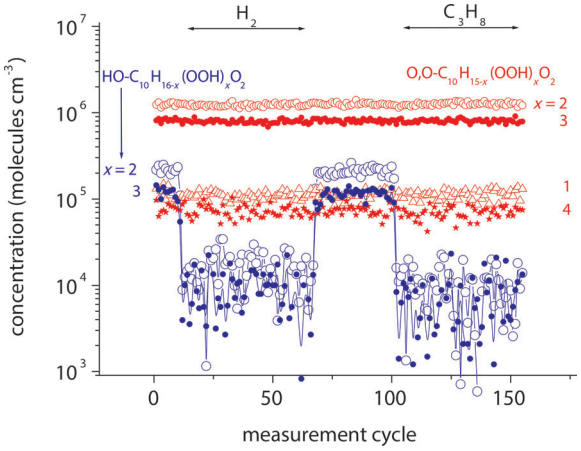

Figure 2. Concentrations of RO_2 radicals in the absence/presence of an OH radical scavenger; [limonene] = 5.0×10^{10}, $[O_3] = 5.8 \times 10^{11}$ molecules cm^{-3}, and if used $[H_2] = 8.2 \times 10^{16}$ or $[C_3H_8] = 1.6 \times 10^{15}$ molecules cm^{-3} scavenging more than 98% of the OH radicals, reaction time: 8.3 s.

The temporal behavior of the RO_2 radicals and the formation of closed-shell products was investigated for close to atmospheric reactant concentrations over a range of reaction times between 8.3 and 39.5 s. Figure 3 depicts the time dependence of the concentration of the O,O-$C_{10}H_{15-x}(OOH)_xO_2$ and HO–$C_{10}H_{16-x}(OOH)_xO_2$ radicals as well as of selected closed-shell monomers and dimers.

All RO_2 radical concentrations increased with time (Figure 3a), whereas the relative concentration ratios were almost constant after about 10 s or even sooner. This demonstrates the fast conversion of an RO_2 radical to the next one on a time scale of a few seconds or less. The complexity of the reaction

 © 2014 Wiley-VCH Verlag GmbH & Co. KGaA, Weinheim

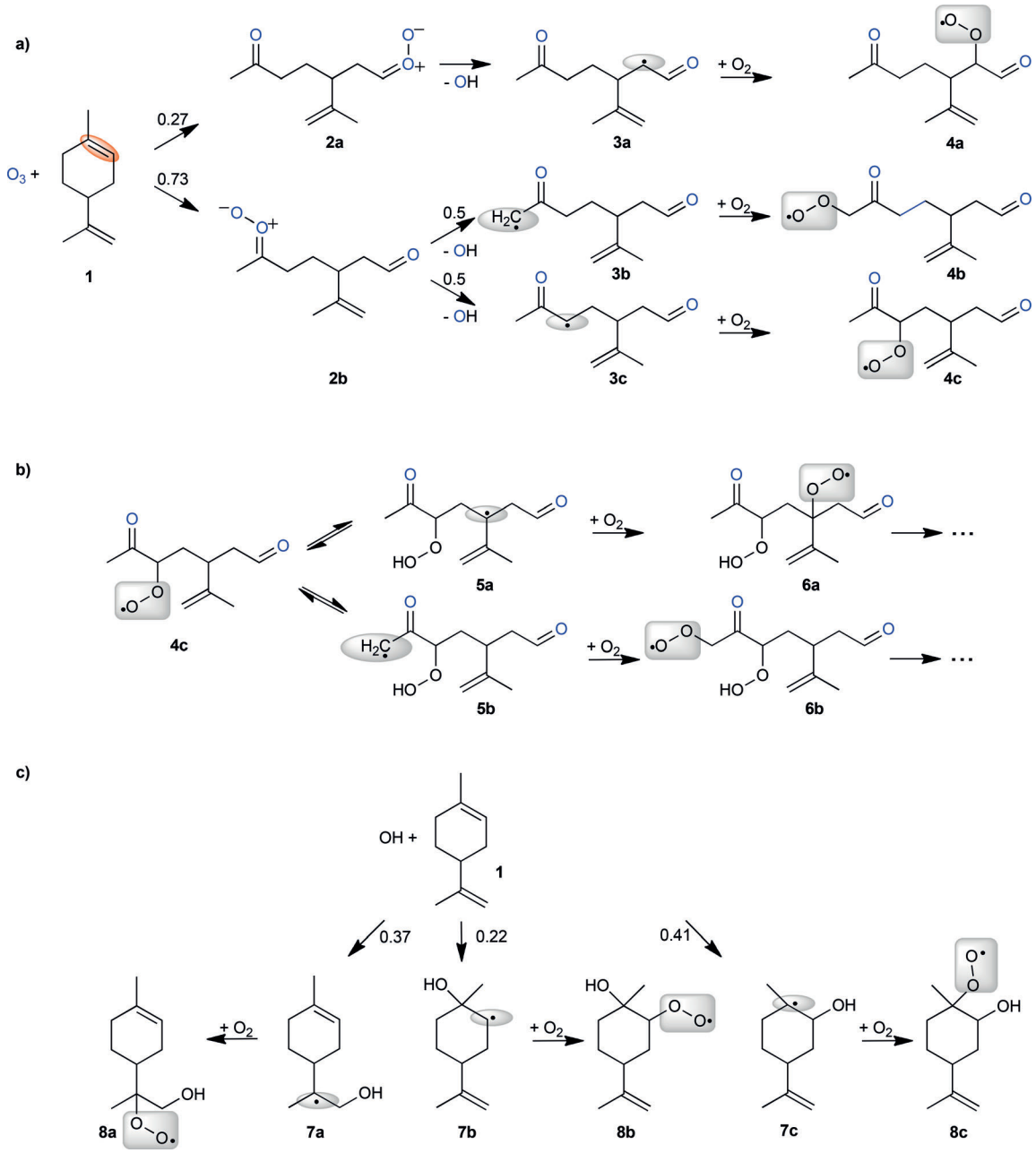

Scheme 1. Formation of RO_2 radicals from the O_3- and OH-initiated oxidation of limonene. a) First steps of ozonolysis, only the O_3 attack at the most reactive, endocyclic double bond is considered.[7,8] b) Example of a reversible intramolecular H-abstraction step (ROO→QOOH) starting from **4c** followed by the subsequent addition of O_2. c) First steps of the OH radical reaction, branching ratios from Ref. [7].

system does not, however, allow a more precise determination of the RO_2 interconversion kinetics.

By changing the O_2 concentration, we tested whether the rate of the back reaction QOOH→ROO (e.g. **5a**→**4c**) can be competitive with the rate of the O_2 addition on QOOH (e.g. **5a** + O_2→**6a**). Notable changes (up to a factor of two) in the RO_2 concentrations were measured when the O_2 concentration was decreased by a factor of three from atmospheric conditions, while reduction of the O_2 concentration by a factor of 300 influenced substantially the product formation (see Figure S4). This observation indicates that even in the atmosphere with $[O_2] = 5.2 \times 10^{18}$ molecules cm^{-3}, the fate of QOOH is not exclusively governed by the reaction with O_2. The rate coefficient of the back reactions, QOOH→ROO, can be on the same order of magnitude as $k_{O_2}[O_2] = 5.2 \times 10^6$ s^{-1} ($k_{O_2} = 10^{-12}$ cm^3 molecule^{-1} s^{-1})[11] for QOOH + O_2→R′O_2. This finding is in line with results from calculations of the rate coefficient for the back reaction which gave of up to 10^8 s^{-1} for different reaction systems.[3a]

The formation of closed-shell monomers (Figure 3b) can formally be explained by a loss of one O atom and one H atom starting from the corresponding O,O-$C_{10}H_{15-x}$-$(OOH)_xO_2$ radical, for example, $C_{10}H_{14}O_7$ from the RO_2 radical with $x = 2$ etc. The loss of one O atom and one H

 © 2014 Wiley-VCH Verlag GmbH & Co. KGaA, Weinheim

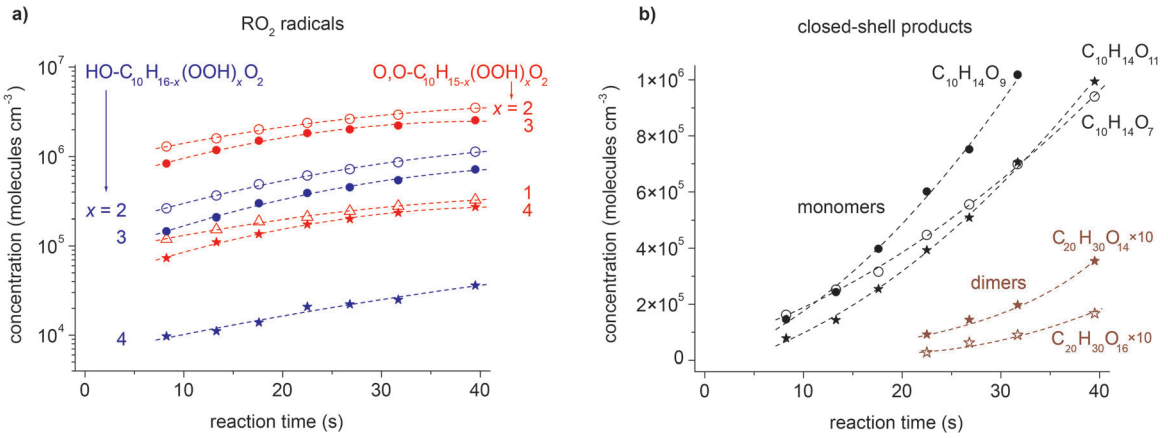

Figure 3. Plot of product formation versus reaction time. a) RO_2 radicals from the ozone ($O,O\text{-}C_{10}H_{15-x}(OOH)_xO_2$ for $x=1$–4) and OH radical reaction ($HO{-}C_{10}H_{16-x}(OOH)_xO_2$ for $x=2$–4); [limonene] $=5.0\times10^{10}$, $[O_3]=5.5\times10^{11}$ molecules cm^{-3}. The signal of $HO{-}C_{10}H_{15}(OOH)O_2$ was too small for a reliable determination of its concentration. b) Most abundant closed-shell products with a C_{10} skeleton (monomers) and a C_{20} skeleton (dimers) from the same measurement series as given in (a); values multiplied by 10.

atom can take place via two routes with it being difficult to deduce conclusively the contributions of the two options to monomer generation based on our findings:

1) a unimolecular reaction in which an OH radical is split off (Scheme S1a)[3a]
2) the reaction of $O,O\text{-}C_{10}H_{15-x}(OOH)_xO_2$ with all other RO_2 radicals, forming $O,O\text{-}C_{10}H_{15-x}(OOH)_xO$. The subsequent reaction of this alkoxy radical with O_2 generates HO_2 and a carbonyl $O,O\text{-}C_{10}H_{14-x}O(OOH)_x$ ($C_{10}H_{14}O_7$, $C_{10}H_{14}O_9$, etc.); decomposition or isomerization of the alkoxy radical can also occur (Scheme S1b).[12]

The formation of the dimers $C_{20}H_{30}O_{14}$ and $C_{20}H_{30}O_{16}$ can be envisaged as the formal dimerization of the corresponding OOH-group-containing RO_2 radicals via the reaction $RO_2 + R'O_2 \rightarrow ROOR' + O_2$. In this context, the most abundant dimer, $C_{20}H_{30}O_{14}$, can be explained as a product of the most abundant OOH-group-containing RO_2 radical, $O,O\text{-}C_{10}H_{13}$-

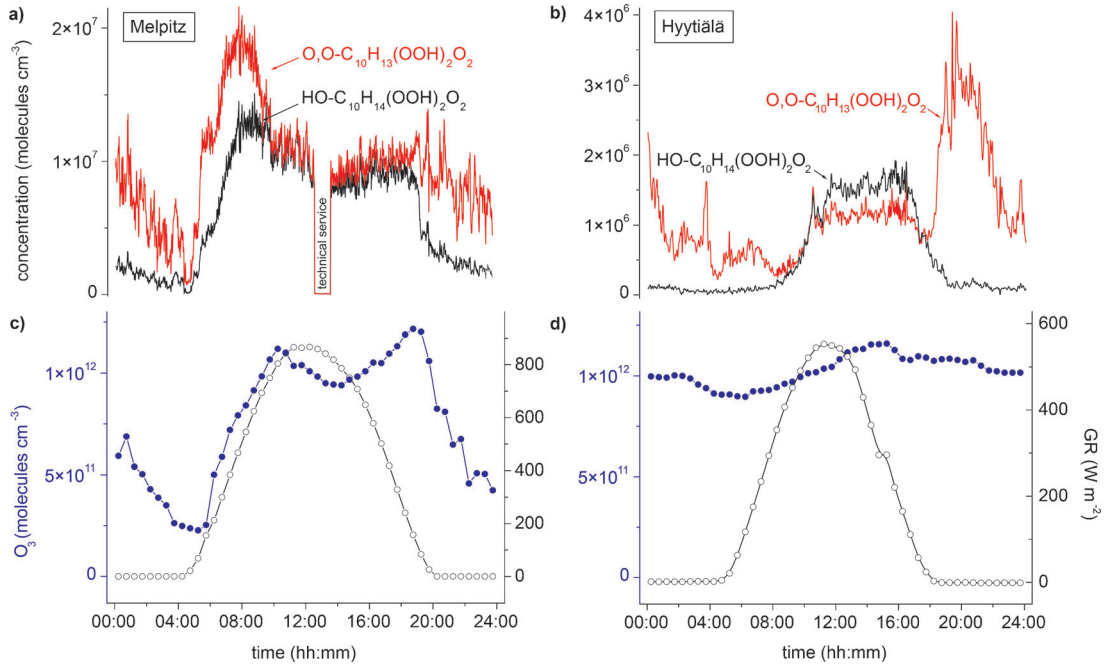

Figure 4. Field measurements in Melpitz (July 21, 2013) and Hyytiälä (March 31, 2011). The measurement sites are close to (Melpitz) or within (Hyytiälä) forested areas. Panels a) and b) show the time series for the most important highly oxidized RO_2 radicals from the ozone- ($O,O\text{-}C_{10}H_{13}(OOH)_2O_2$) and OH-initiated ($HO{-}C_{10}H_{14}(OOH)_2O_2$) reactions of limonene and α-pinene. In panels c) and d) the corresponding concentrations of ozone (blue data points) and the global radiation (black data points) are plotted. Global radiation (GR) stands as a proxy for the OH radical concentration assuming that photochemical OH production dominates. Measurements of highly oxidized RO_2 radicals in Melpitz were carried out with a NO_3^--CI-APi-TOF mass spectrometer as described in this work and in Hyytiälä as described by Jokinen et al.[6]

 © 2014 Wiley-VCH Verlag GmbH & Co. KGaA, Weinheim

$(OOH)_2O_2$ ($C_{10}H_{15}O_8$). From the heavy-ozone experiments, we concluded that these C_{20} dimers contain four O atoms from heavy ozone, supporting the proposed dimer-formation mechanism.

Field measurements at the TROPOS research site in Melpitz,[13] Germany, and the SMEAR II station in Hyytiälä,[14] Finland, were carried out in order to assess the importance of these laboratory findings under atmospheric conditions. All signals identified in our laboratory investigations were also detected in the field measurements. The most abundant, highly oxidized RO_2 radicals, O,O-$C_{10}H_{13}$-$(OOH)_2O_2$ and HO–$C_{10}H_{14}(OOH)_2O_2$, reached peak concentrations of a few 10^7 molecules cm^{-3} (Figure 4a,b). Their concentration profile followed roughly the diurnal behavior of O_3 and OH radicals (Figure 4c,d), depending on the availability of the monoterpenes as the other reactant.

Thus, the results from the field measurements confirm the laboratory findings and prove the importance of the old reaction principle of autoxidation for the oxidation of hydrocarbons in the atmosphere. The formed, highly oxidized RO_2 radicals and, subsequent closed-shell products are expected to have extremely low volatilities. For this reason, they are crucial for the growth of atmospheric aerosols and thereby influence aerosol–cloud–climate interactions. The highly oxidized organic nitrates, detected in high yields from $RO_2 + NO$, are probably important in the formation of new particles as well.[15] Much more experimental work as well as modeling studies are needed for a better understanding of this autoxidation mechanism and its importance for atmospheric processes.

Received: August 27, 2014
Published online: October 29, 2014

Keywords: atmospheric chemistry · autoxidation · mass spectrometry · radical reactions

[1] H. N. Jazukowitsch, *Ber. Dtsch. Chem. Ges.* **1875**, *8*, 766–769.
[2] a) H. Staudinger, *Ber. Dtsch. Chem. Ges.* **1925**, *58*, 1075–1079; b) A. Rieche, *Angew. Chem.* **1937**, *50*, 520–524; c) W. Pritzkow, K. A. Müller, *Justus Liebigs Ann. Chem.* **1956**, *597*, 167–181.
[3] a) J. D. Crounse, L. B. Nielsen, S. Jorgensen, H. G. Kjaergaard, P. O. Wennberg, *J. Phys. Chem. Lett.* **2013**, *4*, 3513–3520; b) J. D. Crounse, H. C. Knap, K. B. Ornso, S. Jorgensen, F. Paulot, H. G. Kjaergaard, P. O. Wennberg, *J. Phys. Chem. A* **2012**, *116*, 5756–5762.
[4] a) M. Ehn, E. Kleist, H. Junninen, T. Petäjä, G. Lönn, S. Schobesberger, M. Dal Maso, A. Trimborn, M. Kulmala, D. R. Worsnop, A. Wahner, J. Wildt, T. F. Mentel, *Atmos. Chem. Phys.* **2012**, *12*, 5113–5127; b) M. Ehn et al., *Nature* **2014**, *506*, 476–479.
[5] T. Berndt, O. Böge, F. Stratmann, J. Heintzenberg, M. Kulmala, *Science* **2005**, *307*, 698–700.
[6] T. Jokinen, M. Sipilä, H. Junninen, M. Ehn, G. Lönn, J. Hakala, T. Petäjä, R. L. Mauldin III, M. Kulmala, D. R. Worsnop, *Atmos. Chem. Phys.* **2012**, *12*, 4117–4125.
[7] MCM. Master Chemical Mechanism, MCMv3.2: http://mcm.Leeds.ac.uk/MCM/ (2014). Last accessed 30. April 2014.
[8] L. Baptista, R. Pfeifer, E. C. da Silva, G. Arbilla, *J. Phys. Chem. A* **2011**, *115*, 10911–10919.
[9] J. H. Kroll, J. S. Clarke, N. M. Donahue, J. G. Anderson, K. L. Demerjian, *J. Phys. Chem. A* **2001**, *105*, 1554–1560.
[10] a) R. Atkinson, S. M. Aschmann, W. P. L. Carter, A. M. Winer, J. N. Pitts, *J. Phys. Chem.* **1982**, *86*, 4563–4569; b) F. Zabel, A. Reimer, K. H. Becker, E. H. Fink, *J. Phys. Chem.* **1989**, *93*, 5500–5507.
[11] P. D. Lightfoot, R. A. Cox, J. N. Crowley, M. Destriau, G. D. Hayman, M. E. Jenkin, G. K. Moortgat, F. Zabel, *Atmos. Environ. Part A* **1992**, *26*, 1805–1961.
[12] S. C. Kwok, J. Arey, R. Atkinson, *J. Phys. Chem. J. Phys. Chem. A* **1996**, *100*, 214–219.
[13] G. Spindler, A. Grüner, K. Müller, S. Schlimper, H. Herrmann, *J. Atmos. Chem.* **2013**, *70*, 165–195.
[14] P. Hari, M. Kulmala, *Boreal Environ. Res.* **2005**, *10*, 315–322.
[15] M. Kulmala et al., *Science* **2013**, *339*, 943–946.

 © 2014 Wiley-VCH Verlag GmbH & Co. KGaA, Weinheim